Pharmacology & Pharmacy, 2025, 16(3), 73-90
https://www.scirp.org/journal/pp
ISSN Online: 2157-9431
ISSN Print: 2157-9423

Determination of Pimavanserin and Its Metabolites in Mouse Plasma Using LC-MS/MS: Investigating Pharmacokinetics Following Different Routes of Administration

Hengxiao Ai[1,2], Lingchao Wang[1], Xia Wu[1], Wenpeng Zhang[1], Haixia Wu[2], Xiaomei Zhuang[1*]

[1]Beijing Institute of Pharmacology and Toxicology, Beijing, China
[2]College of Pharmay, Hebei University of Science and Technology, Shijiazhuang, China
Email: *xiaomeizhuang@163.com

How to cite this paper: Ai, H.X., Wang, L.C., Wu, X., Zhang, W.P., Wu, H.X. and Zhuang, X.M. (2025) Determination of Pimavanserin and Its Metabolites in Mouse Plasma Using LC-MS/MS: Investigating Pharmacokinetics Following Different Routes of Administration. *Pharmacology & Pharmacy*, **16**, 73-90.
https://doi.org/10.4236/pp.2025.163006

Received: February 21, 2025
Accepted: March 16, 2025
Published: March 19, 2025

Abstract

Objective: The aim was to develop a straightforward, efficient, and sensitive LC-MS/MS assay for quantifying pimavanserin (ACP-103) and its active metabolite (N-desmethyl pimavanserin, AC-279) in mouse plasma to assess the pharmacokinetics of ACP-103 following various routes of administration in mice. **Methods:** Mouse plasma samples were prepared using acetonitrile protein precipitation. Chromatographic separation was achieved on a Phenomenex C18 column with a mobile phase consisting of 0.1% formic acid in water (solvent A) and 0.1% formic acid in acetonitrile (solvent B). A total of 54 male mice were divided into nine groups (six per group) and received different doses (0.3, 1, 3 mg/kg) of Pimavanserin tartrate via nasal drip, intramuscular injection, or subcutaneous injection. Venous blood samples were collected at various time points pre- and post-administration, and plasma concentrations of ACP-103 and AC-279 were determined. **Results:** The intra-day and inter-day accuracy for ACP-103 and AC-279 in quality control plasma samples ranged from 90.87% to 105.50%, with precision within 20% and 10%, respectively. Comparative exposure of Pimavanserin tartrate was observed following nasal drip and intramuscular administration, while subcutaneous injection resulted in lower exposure. Increasing doses led to higher drug concentrations for all routes, with no significant differences in AC-279 production. **Conclusion:** The developed LC-MS/MS method was effectively utilized for pharmacokinetic studies in mice after administration of Pimavanserin tartrate at 0.3, 1, and 3 mg/kg via nasal drip, intramuscular injection, and subcutaneous injection. Notable differences in the pharmacokinetic profiles of ACP-103 were observed depending on the route of administration.

*Corresponding author.

Keywords

Pimavanserin, Pharmacokinetics, Mouse, Different Administration Route

1. Introduction

Parkinson's disease (PD) is the second most prevalent neurodegenerative disorder after Alzheimer's disease [1]. It is primarily defined by a constellation of motor symptoms collectively referred to as Parkinsonism, which includes tremors, rigidity, bradykinesia, and postural instability [2]. Data indicates that the incidence of PD in individuals over the age of 65 in China is approximately 1.7%. PDP is a prevalent and severe complication associated with PD, manifesting as hallucinations and/or delusions. The lifetime prevalence of PDP among PD patients is as high as 60%, significantly worsening the condition and impacting the patients' quality of life [3].

Currently, PDP treatment primarily involves pharmacological interventions aimed at symptom relief. The optimal approach to managing PDP typically involves reducing the dosage of antiparkinsonian medications, such as dopamine agonists, and, if necessary, introducing an antipsychotic medication if symptoms persist [4] [5]. Clozapine and quetiapine are frequently utilized in clinical settings due to their ability to alleviate psychotic symptoms without exacerbating motor issues [6] [7]. However, clozapine's use is restricted due to potential severe side effects, including granulocytopenia, hypotension, excessive salivation, and pronounced sedation [8]-[10]. Quetiapine, while also effective, can cause hypotension and significant sedation, and is often poorly tolerated by patients [9] [11]. As of April 2016, no clinically safe, effective, and well-tolerated drugs specifically for PDP were available on the market.

Pimavanserin (Nuplazid), a highly selective inverse agonist of the 5-hydroxytryptamine subtype 2A receptors, offers a unique advantage by targeting the 5-HT_{2A} receptors without affecting dopamine receptors. This selectivity helps to avoid the side effects associated with dopamine receptor activation, such as involuntary tremors, which are common with many schizophrenia medications. In the pivotal Phase III Study-020, Nuplazid was shown to significantly decrease the frequency and severity of psychotic symptoms compared to a placebo, without adversely affecting motor function [12]. Consequently, the U. S. Food and Drug Administration (FDA) granted the drug approval for the treatment of Parkinson's disease psychosis with "Breakthrough Therapy" designation and "Priority Review" [13] [14]. Pimavanserin tablets were released in April 2016 and, at that time, were not yet accessible in China.

In the context of treating PDP, the importance of comparing different routes of administration is particularly significant. Considering the clinical profile of the PD patient population with psychiatric comorbidities, there are several challenges associated with long-term oral medication use: 1. Dysphagia is prevalent, affecting

13% of individuals aged 65 and older and a staggering 51% of those in nursing homes [15]. Additionally, 38.74% of PD patients exhibit dysphagia symptoms [16]. 2. Patients often experience significant mood swings, which can lead to non-compliance with medication regimens and poor adherence to self-administered medication schedules. 3. Pimavanserin's oral absorption is relatively slow, with a T_{max} ranging from 4 to 24 hours in humans and exhibiting considerable inter-individual variability [17]. Furthermore, the decline in drug absorption and metabolic capacity among elderly patients may lead to unstable therapeutic efficacy or increased side effects of oral medications. Therefore, exploring alternative routes of administration (such as nasal spray, intramuscular injection, and subcutaneous injection) not only enhances medication adherence but also optimizes drug absorption and distribution, thereby better addressing the therapeutic needs of elderly PDP patients.

Emphasizing the suitability of administration routes for elderly PD patients is one of the key focuses of this study. Given the unique physiological and pathological conditions of elderly PD patients, developing administration methods tailored to their needs is of significant importance. For instance, nasal spray administration can bypass gastrointestinal absorption and rapidly enter the systemic circulation, making it suitable for patients with dysphagia. Meanwhile, intramuscular and subcutaneous injections can provide more stable drug release and reduce inter-individual variability. These alternative administration routes not only enhance the bioavailability of drugs but also mitigate the risk of treatment interruption due to the inconvenience of oral administration, thereby improving the overall therapeutic outcomes and quality of life for patients.

In this study, we aim to develop and validate a rapid, sensitive LC-MS/MS method for the simultaneous quantification of pimavanserin and its active metabolite in mouse plasma. We will apply this method to pharmacokinetic studies of the parent drug and its active metabolite in mice following administration via nasal drip, intramuscular injection, and subcutaneous injection. The goal is to provide a foundational reference for the development of diverse dosage forms of pimavanserin tailored to the specific needs of this patient population.

2. Experimental Methods

2.1. Reagents and Drugs

Pimavanserin tartrate (pimavanserin tartrate, 99.27% purity) was purchased from Shanghai Taoshu Biotechnology Co. Ltd. Pimavanserin (ACP-103, purity 99.00%), AC-279 (purity 98.00%), verazolidone hydrochloride (internal standard, is; purity 98.00%) were obtained from Shanghai Jizhi Biochemical Technology Co. Ltd. Dimethyl sulfoxide (DMSO) was supplied by Sigma, USA. Formic acid was purchased from J&K Scientific, Beijing, China. Acetonitrile and methanol were purchased from Thermo Fisher Scientific, USA. Pure water was purchased from Hangzhou Wahaha Group Co. Ltd.

2.2. Animals

Healthy male C57BL/6J mice, weighing 19 - 21 g, were purchased from Beijing Viton Lever Technology Co., Ltd, which holds Laboratory Animal Production License No.: SCXK (Beijing) 2016-0001. The experimental animals were housed in a well-ventilated room that was air-conditioned to maintain a stable temperature of 16 to 26 degrees Celsius, relative humidity levels between 40% and 70%, and a light/dark cycle of 12 hours each. All mice were provided with the same standardized diet during the experimental period to ensure consistency in dietary composition and intake, thereby avoiding potential dietary variations that could influence drug metabolism. Throughout the experimental procedures, efforts were made to minimize stress stimuli on the mice, ensuring gentle and consistent handling. All mice were derived from the C57BL/6J strain, which is widely used in pharmacokinetic studies due to its consistent genetic background, thereby reducing the impact of genetic variability on the results. Prior to the experiment, all mice underwent health examinations to ensure the absence of any diseases or abnormal conditions. During the experiment, the health status of the mice was closely monitored, and any individuals exhibiting abnormalities were promptly excluded from the study. The above animal experiments were approved by the Experimental Animal Ethics Committee of the Institute for Medical Research of the Military Academy of Sciences (IACUC-DWZX-2024-P679).

2.3. LC-MS/MS Method

Mass Spectrometry Method: The analysis was performed using Electrospray Ionization (ESI) in combination with Multiple Reaction Monitoring (MRM) in positive ion mode. The collision gas (CAD) was set at 7 psi; the curtain gas (CUR) at 35 psi; the nebulizing gas (GS1) at 55 psi; and the heating gas (GS2) also at 55 psi. The ionization voltage (IS) was 4500 V, and the temperature was maintained at 550˚C. The MS conditions for detecting ACP-103, AC-279, and vilazodone hydrochloride, including their respective second-level MS maps, are detailed in **Table 1** and illustrated in **Figure 1**. The specific mass transitions were as follows: ACP-103 (m/z 428.2 → 223.4), AC-279 (m/z 414.4 → 209.3), and vilazodone hydrochloride (m/z 442.3 → 155.3).

Table 1. Mass spectrometry detection conditions for ACP-103, AC-279, and vilazodone hydrochloride.

chemical compound	ESI	m/z		CE/eV	DP/eV	EP/eV	CXP/eV
		Precursor Ion	Product Ion				
ACP-103	+	428.2	223.4	24	150	10	16
AC-279	+	414.4	209.3	20	180	10	16
Vilazodone hydrochloride (IS)	+	442.3	155.3	60	260	10	16

Chromatographic Method: Separations were achieved using a Phenomenex C18 column (3.0 mm × 50 mm, 2.6 μm) with a mobile phase consisting of a mix-

ture of 0.1% formic acid in water (solvent A) and 0.1% formic acid in acetonitrile (solvent B). The gradient elution program was optimized as follows: 10% B from 0.0 to 0.3 min; a linear increase to 90% B between 0.3 and 1.2 min; holding at 90% B until 2.2 min; a decrease back to 10% B between 2.2 and 2.3 min; and finally, maintaining 10% B from 2.3 to 3.0 min. The flow rate was set at 0.5 mL/min, the column temperature was controlled at 40˚C, and the injection volume was 1 μL.

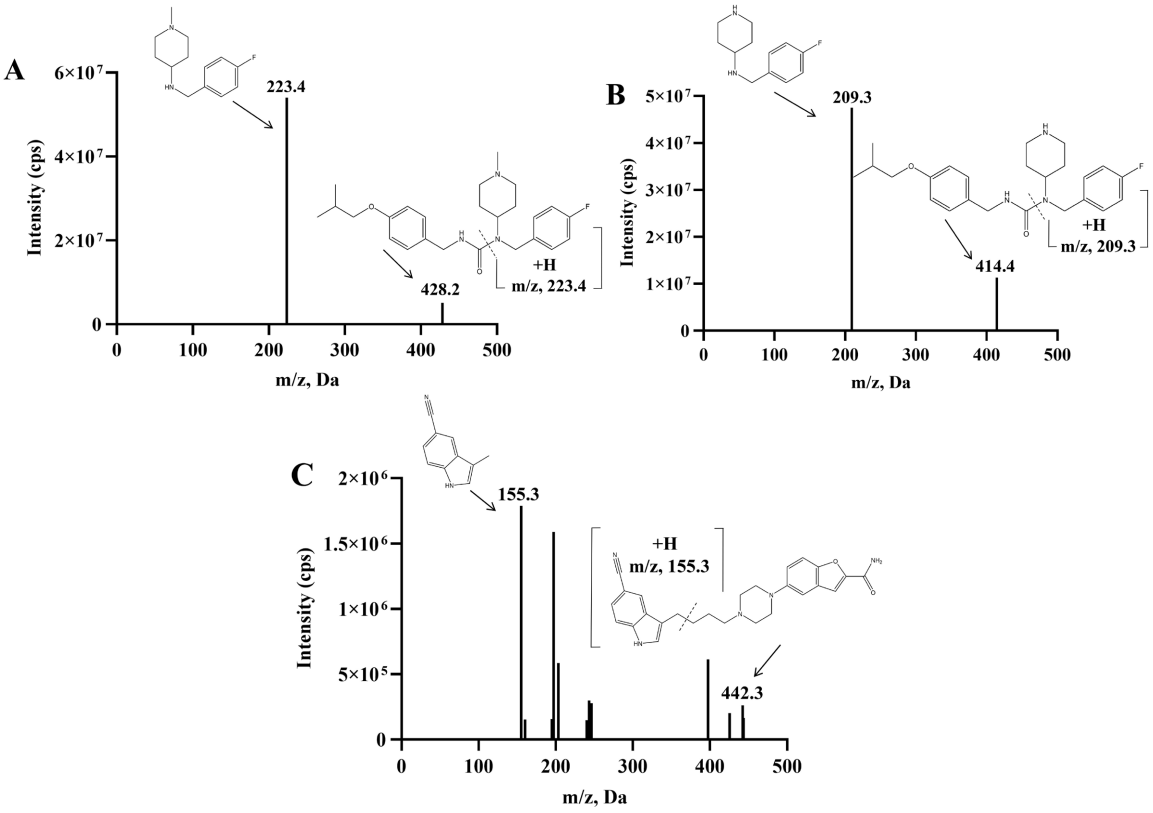

Figure 1. Secondary mass spectra of ACP-103 (A), AC-279 (B), and vilazodone hydrochloride (C).

2.4. Sample Processing

Plasma samples were processed using the protein precipitation method. The procedure began with the aliquoting of 10 μL of mouse plasma into a tube. Then, 10 μL of acetonitrile was added, followed by the introduction of 50 μL of an acetonitrile solution containing the internal standard, vilazodone hydrochloride, at a concentration of 100 ng/mL. The mixture was vortexed for 1 minute to ensure thorough mixing. Subsequently, the samples were centrifuged at 14,000 × g for 10 minutes to precipitate proteins. After centrifugation, 40 μL of the supernatant was carefully transferred and combined with 40 μL of a 50% acetonitrile solution, and the mixture was vortexed again to facilitate further dilution and solubilization. The resulting solution was then ready for analysis.

2.5. Methodological Validation

The method was validated in accordance with the ICH M10 guideline [18].

2.5.1. Selectivity

To evaluate the selectivity of the method, chromatograms were compared across different samples. These included blank plasma from six C57BL/6J mice, plasma samples spiked with ACP-103, AC-279 standards, and the internal standard (IS), as well as plasma samples collected from mice after various routes of ACP-103 administration. This comprehensive comparison ensured that the analytical method was free from endogenous interferences and could accurately quantify the target compounds in biological matrices.

2.5.2. Calibration Curve and Lower Limit of Quantification

Based on the blood concentration data from the preliminary pharmacokinetic studies in C57BL/6J mice, it was established that the calibration curves for ACP-103 and AC-279 in the plasma of these mice were linear over the concentration range of 0.5 to 200 ng/mL. To construct these curves, 10 μL of blank mouse plasma was spiked with 10 μL of a mixed working solution containing known concentrations of ACP-103 and AC-279. This spiking process resulted in target concentrations of 0.5, 1, 2, 5, 10, 20, 50, 100 and 200 ng/mL for both compounds in the mouse plasma. Additionally, double-blank plasma samples (DB) and plasma samples containing only the internal standard (CB) were prepared to serve as controls. The resulting calibration curves demonstrated high correlation coefficients with $r \geq 0.99$, indicating excellent linearity. The lower limit of quantification (LLOQ) was characterized by a relative standard deviation (RSD) ≤ 20% and a relative error (RE) within ± 20%, which is acceptable for initial method validation. For the remaining concentration points, the RSD was ≤ 15% and the RE was within ± 15%, confirming the precision and accuracy of the method across the tested concentration range. These specifications ensure that the assay is robust and suitable for the quantification of ACP-103 and AC-279 in the plasma samples of C57BL/6J mice

2.5.3. Precision and Accuracy

Quality control (QC) samples containing ACP-103 and AC-279 at low, medium, and high concentrations (0.5, 1.5, 15 and 150 ng/mL) were prepared in mouse plasma (n = 6). These samples were analyzed across 3 analytical batches (n = 18), with standard curves included to assess both intra-batch and inter-batch precision (RSD) and accuracy (RE). The validation criteria were set as follows: for the lower limit of quantification (LLOQ), RSD should be ≤ 20% and RE within ± 20%; for the other QC samples, RSD should be ≤ 15% and RE within ± 15%.

2.5.4. Extraction Recovery and Matrix Effect

To assess the matrix effect, 10 μL of blank mouse plasma from 6 different individuals was spiked with 10 μL of a mixed working solution of ACP-103 and AC-279 to achieve low and high QC concentrations of 1.5 and 150 ng/mL (n = 6), respectively. After protein precipitation, the peak areas of ACP-103 and AC-279 were determined. For comparison, the same volume of purified water was used in place of blank plasma, following the same sample preparation procedure, and the peak

areas of ACP-103 and AC-279 were measured. The matrix effect was calculated as the ratio of the peak areas of ACP-103 and AC-279 in plasma samples to those in pure water samples.

For the recovery assessment, plasma from six different individual blank mice was pooled in equal volumes. From this pooled plasma, 10 μL was taken and spiked with 10 μL of the working solutions of ACP-103 and AC-279 to achieve low, medium, and high QC concentrations of 1.5, 15 and 150 ng/mL (n = 6). The samples were then processed before and after protein precipitation to obtain the peak area ratios of ACP-103 and AC-279. Extraction recoveries were calculated based on these peak area ratios. This process allowed for the evaluation of the efficiency of the protein precipitation method in isolating the analytes from the plasma matrix.

2.5.6. Stability

Blank mouse plasma was prepared at low, medium, and high quality control concentrations of 1.5, 15 and 150 ng/mL (n = 3). The stability of the drug-containing plasma samples was assessed through various storage conditions: at room temperature for 4 hours, at 4˚C for 4 hours, at −40˚C for 7 days, after three cycles of repeated freezing and thawing at −40˚C, and for 24 hours at −40˚C in the sample compartment following deproteinization of the plasma samples.

2.5.7. Dilution Linearity and Carry Over

Since the drug concentration in plasma, collected at certain time points after high-dose administration via nasal and intramuscular injections in mice, exceeded the upper limit of quantification of the ACP-103 calibration curve, the accuracy of the dilution of mouse plasma samples was verified. A 500 ng/mL plasma sample (n = 6) was prepared using blank mouse plasma and diluted 10-fold to achieve a concentration of 50 ng/mL.

Carry over: Immediately following the injection of the ULOQ (Upper Limit of Quantification) sample, a blank mouse plasma sample was injected. The peak area ratios of ACP-103, AC-279, and the internal standard in the blank sample were compared to those of ACP-103, AC-279, and vilazodone hydrochloride in the LLOQ (Lower Limit of Quantification) sample.

2.6. Pharmacokinetic Study in Mice

Male mice (C57BL/6J, 19 - 21 g) were randomly assigned to 6 groups, with 6 mice in each group [19]. Pimavanserin tartrate was administered at three different doses (0.3, 1 and 3 mg/kg) via nasal drip, intramuscular injection, and subcutaneous injection, each in a single dose. Blood samples were collected intravenously at time points of 0.033, 0.083, 0.25, 0.5, 1, 2, 4, 6, 8 and 12 hours post-administration of pimavanserin tartrate. Each blood sample volume was 30 μL, placed in heparinized centrifuge tubes, and centrifuged at 2500 × g for 5 minutes to obtain plasma samples, which were then stored at −40˚C for subsequent analysis. The administration volume for plasma samples was 0.4 mL/kg via nasal drip and 5

mL/kg via intramuscular and subcutaneous injection.

2.7. Statistical Analysis

Sample concentrations were determined from the respective standard curves using the LC-MS/MS instrument software. The plasma pharmacokinetic parameters for ACP-103 and AC-279 in mice were calculated employing the non-compartmental analysis (NCA) model in WinNonlin 8.1 software. Data plotting was conducted with GraphPad Prism 8 software. Statistical analyses were carried out using SPSS software, with all measurements expressed as Mean ± SD. For comparisons between groups, ANOVA and t-tests were utilized for statistical evaluation, and significant differences were defined as p-values less than 0.05.

3. Results and Discussions

3.1. Method Selectivity

Figure 2 displays the chromatograms of blank mouse plasma, mouse plasma spiked with ACP-103, AC-279, and the internal standard vilazodone hydrochloride, as well as plasma samples containing the drug post-administration. The retention time for ACP-103 in mouse plasma is 1.64 minutes; for AC-279, it is 1.63 minutes; and for the internal standard vilazodone hydrochloride, it is 1.51 minutes. A baseline separation was achieved, indicating excellent selectivity.

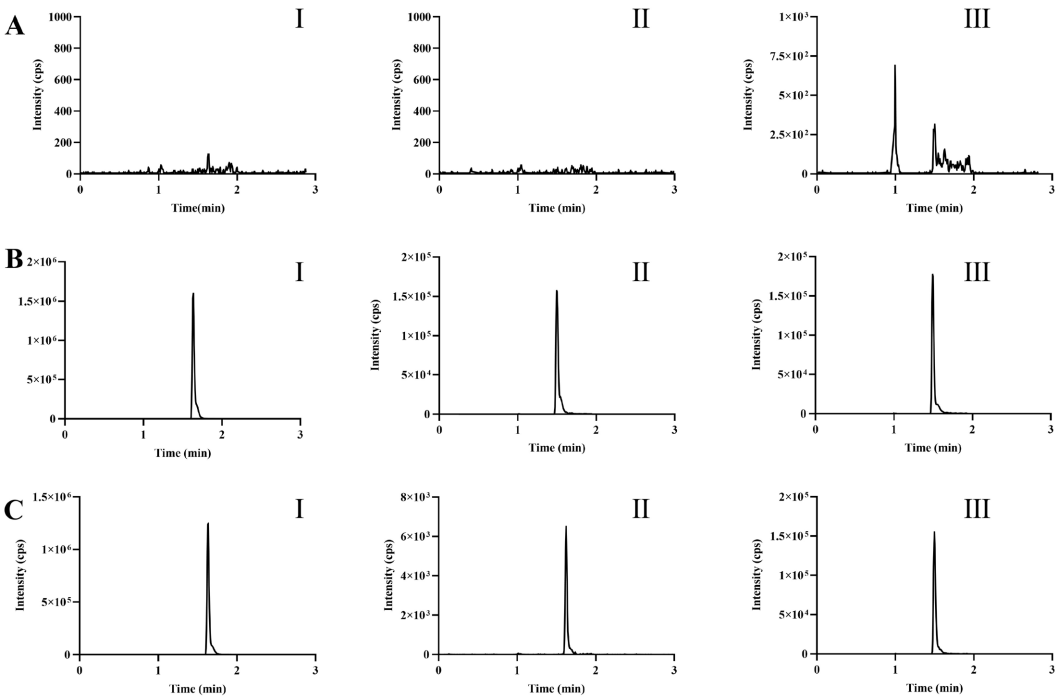

Note: A: Blank mouse plasma sample; B: Blank mouse plasma plus a sample of the mixed working solution of 200 ng/mL ACP-103 and AC-279; C: Plasma sample of mice after intramuscular injection of pimavanserin tartrate (3 mg/kg) for 15 min.

Figure 2. Representative chromatograms of ACP-103 (I), AC-279 (II) and vilazodone hydrochloride (III) in mouse plasma samples.

3.2. Calibration Curve and Lower Limit of Quantification

The corresponding calibration curves were derived following weighted ($1/X^2$) regression analysis, with the concentrations of ACP-103 and AC-279 (in ng/mL) plotted on the horizontal axis and the ratio of the peak areas of ACP-103 and AC-279 to that of vilazodone hydrochloride, the internal standard, on the vertical axis. The resulting linear equations were Y = 0.0511X + 0.00957 (with a correlation coefficient r = 0.9964) for ACP-103, and Y = 0.0172X + 0.00116 (with a correlation coefficient r = 0.9957) for AC-279. These linear relationships indicate a strong correlation, as depicted in Figure 3.

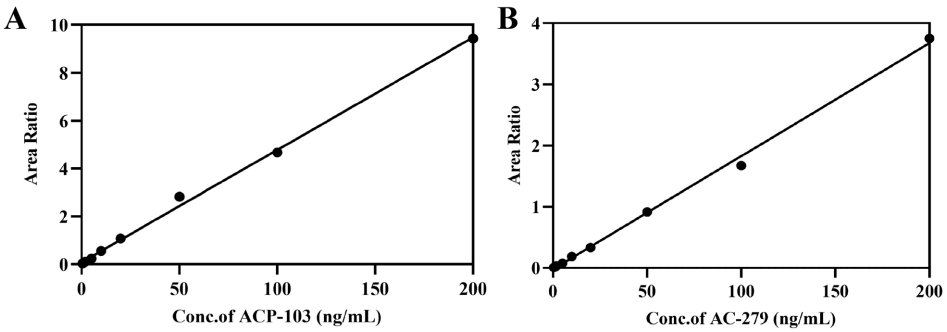

Figure 3. Calibration curves of ACP-103 (A) and AC-279 (B) in mouse plasma samples.

3.3. Precision and Accuracy

LLOQ for ACP-103 in mouse plasma showed intra-day and inter-day accuracy ranging from 97.43% to 101.99%, and precision within 20%. For AC-279 in mouse plasma, the LLOQ demonstrated intra-day and inter-day accuracy between 93.62% and 100.59%, with precision within 10%, satisfying the methodological requirements. The intra-day and inter-day accuracy for AC-279 in mouse plasma was within the range of 103.42% to 105.50%, and the precision was within 10%. The accuracies for the other quality control (QC) samples were within 93.62% to 100.59%, and the precision was within 10%, as presented in Table 2. These results comply with the established methodological criteria.

Table 2. Precision and accuracy of ACP-103 and AC-279 in mouse plasma.

Analytes	Concentration (ng/mL)	Intra-day (n = 6)		Intra-day (n = 18)	
		Accuracy (%)	RSD (%)	Accuracy (%)	RSD (%)
ACP-103	0.5	97.43 ± 9.80	10.06	101.99 ± 9.98	9.79
	1.5	90.87 ± 7.70	8.47	93.68 ± 6.13	6.54
	15	104.67 ± 10.72	10.24	99.78 ± 8.59	8.61
	150	102.13 ± 12.53	12.27	99.05 ± 7.61	7.68
AC-279	0.5	105.5 ± 4.04	3.83	103.42 ± 6.41	6.20
	1.5	93.62 ± 7.94	8.48	97.92 ± 8.25	8.43
	15	99.45 ± 9.79	9.84	100.16 ± 7.66	7.65
	150	95.62 ± 7.44	7.78	100.59 ± 6.81	6.77

3.4. Extraction Recovery and Matrix Effects

The extraction recoveries of ACP-103 and AC-279 in mouse plasma, at low, medium, and high concentrations, were found to be within the range of 96.10% to 102.64%. The matrix effects for ACP-103 and AC-279 were 98.55% to 101.23% and 100.00% to 102.06%, respectively, indicating no significant matrix effect. The specific data are detailed in Table 3, confirming that the methodology fulfills the requirements.

Table 3. Extraction recoveries and matrix effects of ACP-103 and AC-279 in mouse plasma (n = 6).

Analytes	concentration (ng/mL)	Extraction recovery (%)	Matrix effect (%)	Matrix effect RSD (%)
ACP-103	1.5	99.30 ± 5.54	98.55 ± 5.57	5.65
	15	98.74 ± 3.96	-	-
	150	102.64 ± 2.54	101.23 ± 5.15	5.09
AC-279	1.5	99.42 ± 11.39	100.00 ± 13.35	13.35
	15	96.10 ± 6.14	-	-
	150	102.12 ± 4.31	102.06 ± 1.91	1.87

3.5. Stability

When comparing the prepared QC samples with freshly prepared QC samples after storage under various conditions, the accuracy of the ACP-103 stability samples was within 90.53% to 103.77%, with precision (RSD) within 13.24%. Similarly, the accuracy of the AC-279 stability samples was within 86.97% to 103.63%, and the precision (RSD) was within 8.48%. These results demonstrate that both ACP-103 and AC-279 are stable under the tested conditions, as shown in Table 4. The precision (RSD) for all samples was within 8.61%, confirming the stability of ACP-103 and AC-279 under the specified conditions, with the specific data presented in Table 4.

Table 4. Stability of ACP-103, AC-279 in mouse plasma under various conditions (Mean ± SD, n = 3).

Analytes	Concentration (ng/mL)	Room temperature for 24 h		4˚C for 24 h		In auto-sampler for 24 h		Freeze-thaw three times		−40˚C for 7 d	
		Accuracy %	RSD %	Accuracy %	RSD %	Accuracy %	RSD %	Accuracy %	RSD %	Accuracy %	RSD %
ACP-103	1.5	95.67 ± 1.47	1.54	101.63 ± 7.63	7.51	92.33 ± 7.41	8.03	93.43 ± 0.90	0.96	96.53 ± 9.68	10.03
	15	96.77 ± 8.16	8.43	91.70 ± 2.91	3.17	90.53 ± 7.22	7.98	94.97 ± 6.46	6.80	95.07 ± 4.43	4.66
	150	97.37 ± 8.03	8.25	103.77 ± 9.12	8.79	102.90 ± 13.62	13.24	100.13 ± 8.55	8.54	92.67 ± 5.41	5.84
AC-279	1.5	89.67 ± 3.18	3.55	92.90 ± 5.47	5.89	90.20 ± 2.78	3.08	86.97 ± 0.47	0.54	88.2 ± 0.75	0.85
	15	96.47 ± 5.28	5.47	92.43 ± 6.67	7.22	93.67 ± 6.25	6.67	96.17 ± 5.95	6.19	90.00 ± 1.61	1.79
	150	95.53 ± 4.83	5.06	103.63 ± 7.41	7.15	102.3 ± 8.68	8.48	103.33 ± 7.64	7.39	95.63 ± 4.1	4.29

3.6. Dilution Linearity and Carry Over

Dilution linearity: Mouse whole blood samples, after being taken, were centrifuged to obtain supernatants, which were then diluted 10-fold. The accuracy of both ACP-103 and AC-279 in mouse plasma was found to be within the range of 85% to 115%, meeting the methodological requirements, as illustrated in Table 5.

Carry over: Blank samples were analyzed immediately following the analysis of ULOQ samples. For the analytes ACP-103, AC-279, and vilazodone hydrochloride, no peaks were observed in the blank samples that exceeded 20% of the LLOQ. This indicates that the method is suitable for determining samples with unknown concentrations, as it demonstrates negligible carry-over effects.

Table 5. Dilution linearity of ACP-103, AC-279 in mouse plasma (Mean ± SD, n = 6).

Analytes	Diluted 10 times (ng/mL)	Accuracy (%)
ACP-103	49.62 ± 1.88	99.20 ± 3.79
AC-279	49.15 ± 2.73	98.28 ± 5.46

3.7. Comparison of Pharmacokinetics in Mice with Different Routes of Administration of ACP-103

The mean drug-time curves in plasma and the principal pharmacokinetic parameters for mice following administration of ACP-103 at varying doses (0.3, 1 and 3 mg/kg) through nasal drip, intramuscular injection, and subcutaneous injection are depicted in Figures 4-5 and detailed in Table 6. Mice that received pimavanserin tartrate via different administration routes exhibited distinct drug exposure profiles: the nasal drip administration of ACP-103 resulted in the highest drug exposure and the briefest residence time; whereas, the subcutaneous administration of ACP-103 showed the lowest exposure and the most extended residence time. ACP-103 administered via nasal drip demonstrated the highest exposure and the shortest residence time in vivo, whereas ACP-103 given via subcutaneous injection displayed the lowest exposure and the longest residence time in vivo. With varying doses post-administration, all three routes displayed an increasing trend in drug concentration. However, the nasal drip route offered the most linear drug exposure, and both intramuscular and subcutaneous injections exhibited a disproportionate and significant increase as the dose increased.

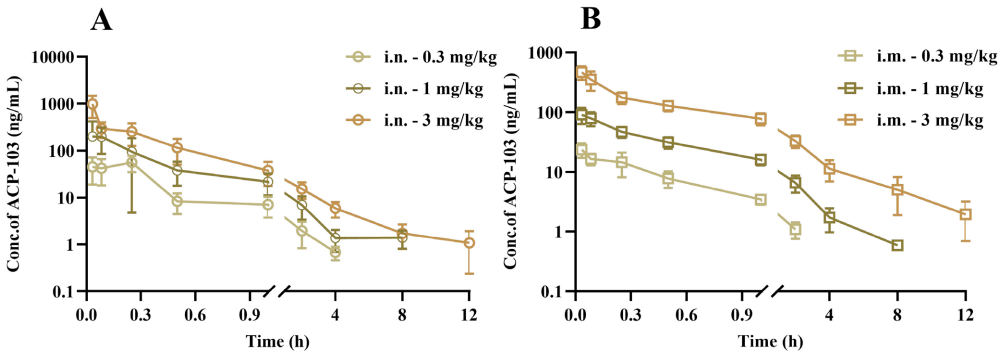

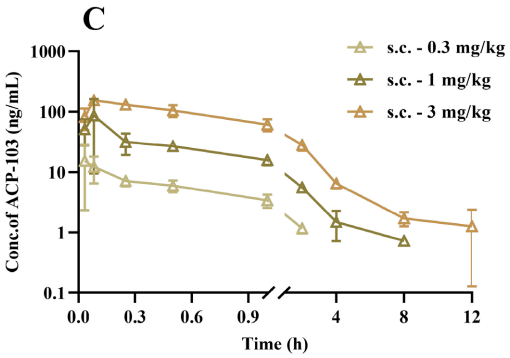

Note: A: nasal drip; B: intramuscular injection; C: subcutaneous injection

Figure 4. Mean concentration-time curves of pimavanserin after administrated to mice by different routes across different doses (Mean ± SD, n = 6).

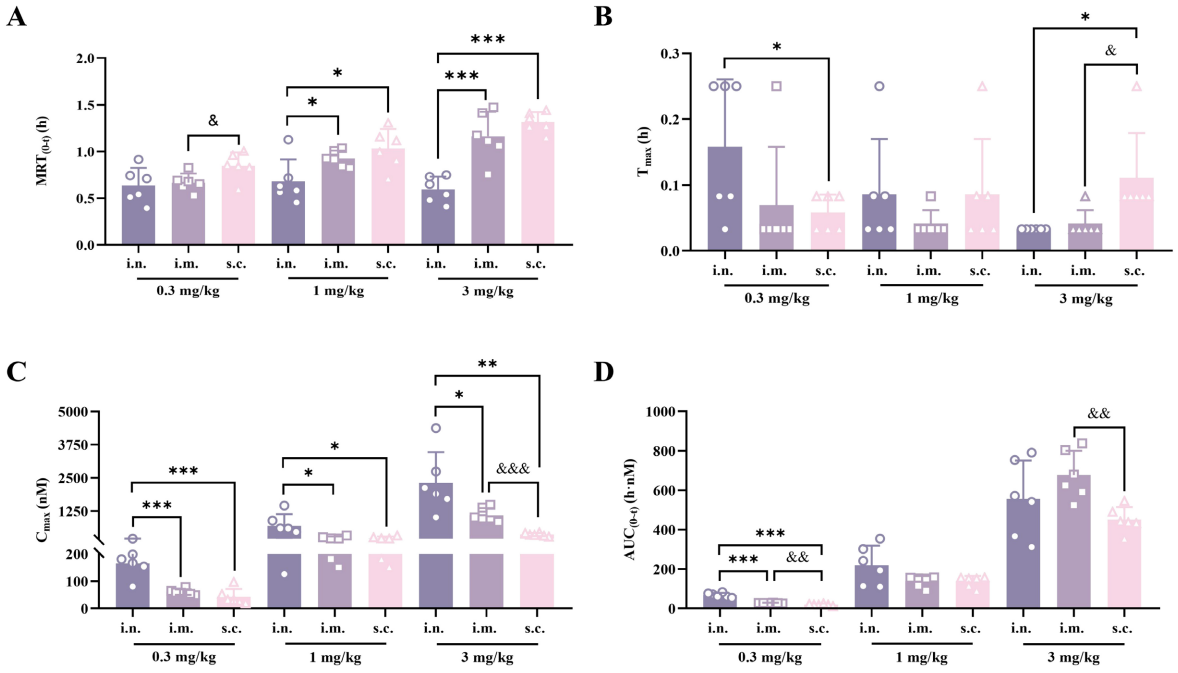

Figure 5. Comparison of major pharmacokinetic parameters of ACP-103 in mice after administration of pimavanserin tartrate by different routes (Mean ± SD, n = 6).

Table 6. Main pharmacokinetic parameters of ACP-103 in mice after administration of pimavanserin tartrate by different routes (Mean ± SD, n = 6).

Parameters	Unit	i. n.			i. m.			s. c.		
		0.3	1	3	0.3	1	3	0.3	1	3
$t_{1/2}$	h	0.86 ± 0.42	0.90 ± 0.30	1.58 ± 0.73	0.55 ± 0.09	0.93 ± 0.18	1.5 ± 0.34	0.61 ± 0.07	0.98 ± 0.25	1.02 ± 0.15$^{\&}$
C_{max}	nM	164.60 ± 45.75	687.0 ± 449.0	2309 ± 1156	60.39 ± 10.36***	226.32 ± 62.27*	1091 ± 272*	43.07 ± 28.87***	220.19 ± 171.54*	363.74 ± 60.$^{94**, \&\&\&}$
T_{max}	h	0.16 ± 0.1	0.09 ± 0.08	0.03 ± 0	0.07 ± 0.09	0.04 ± 0.02	0.04 ± 0.02	0.06 ± 0.03*	0.09 ± 0.08	0.11 ± 0.07$^{*, \&}$
C_{max}/Dose	nM × kg/mg	548.67 ± 152.50	686.98 ± 449	769.72 ± 385.39	201.3 ± 34.52	226.32 ± 62.27	363.61 ± 90.58$^{\#\#}$	143.57 ± 96.24	220.19 ± 171.54	121.25 ± 20.31

Continued

$AUC_{(0-t)}$	h × nM	67.79 ± 11.14	219.28 ± 99.34	555.63 ± 194.73	27.94 ± 1.31$^{\&\&\&}$	137.53 ± 27.96	676.69 ± 122.71	20.24 ± 4.65$^{***,\&\&}$	115.63 ± 32.93	450.40 ± 63.93$^{\&\&}$
$AUC_{(0-\infty)}$	h × nM	73.16 ± 16.04	222.96 ± 99.78	560.77 ± 197.01	30.03 ± 1.82	141.23 ± 29.12	689.79 ± 133.26	22.96 ± 4.45	122.55 ± 30.26	454.98 ± 64.22
$MRT_{(0-t)}$	h	0.64 ± 0.19	0.68 ± 0.24	0.59 ± 0.14	0.67 ± 0.10	0.92 ± 0.09*	1.16 ± 0.26***	0.85 ± 0.14$^{\&}$	1.03 ± 0.21*	1.32 ± 0.11***
$AUC_{(0-t)}$/Dose	h × nM × kg/mg	225.96 ± 37.13	219.28 ± 99.34	185.21 ± 64.91	93.13 ± 4.37	137.53 ± 27.96$^{\#\#}$	225.56 ± 40.90$^{\#\#\#}$	67.47 ± 15.51	115.63 ± 32.93$^{\#\#}$	150.13 ± 21.31$^{\#\#\#}$

$^{\#\#}P < 0.01$; $^{\#\#\#}P < 0.001$ compared with the low dose group. $^{*}P < 0.05$; $^{**}P < 0.01$; $^{***}P < 0.001$, same dose compared with nasal drip. $^{\&}P < 0.05$; $^{\&\&}P < 0.01$; $^{\&\&\&}P < 0.001$, at the same dose compared with intramuscular injection.

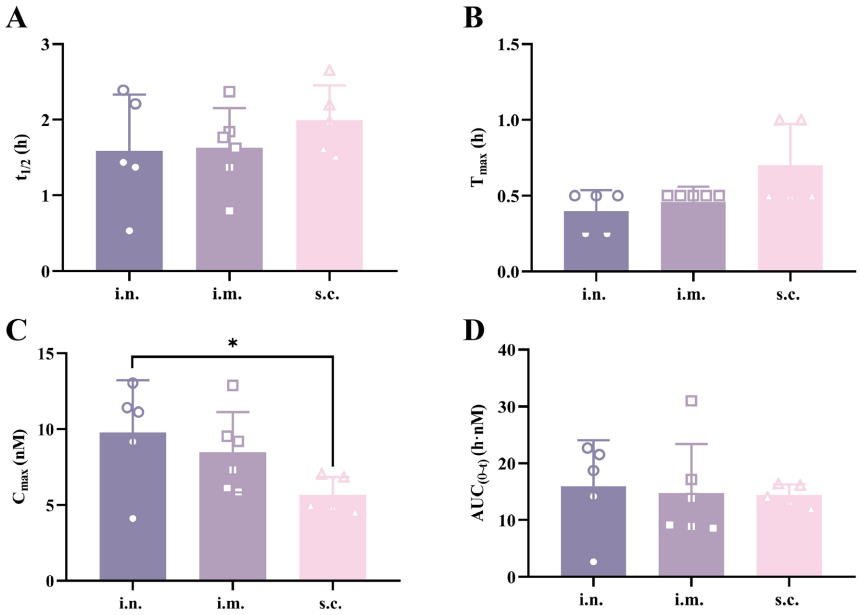

Figure 6. Comparison of major pharmacokinetic parameters of AC-279 in mice after administration of pimavanserin tartrate by different routes (Mean ± SD, n = 6).

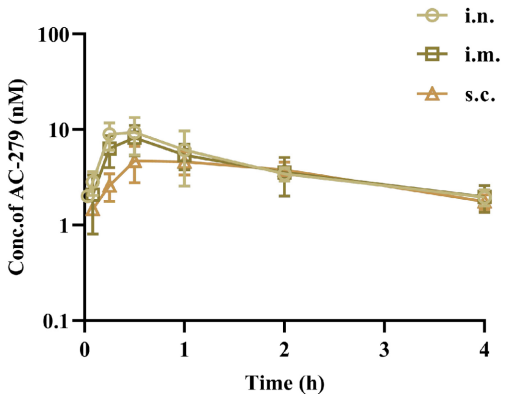

Figure 7. Concentration-time curves of AC-279 in mice after administration of pimavanserin tartrate (3 mg/kg) by different route (Mean ± SD, n = 6).

For the metabolite AC-279, the active metabolite was detectable only after administration of a high dose of pimavanserin tartrate (3 mg/kg) via different routes,

with a low product generation rate. The plasma mean drug-time curves and the main pharmacokinetic parameters are presented in Figures 6-7 and Table 7. The results indicated that among the three administration routes, the in vivo residence time of AC-279 was the shortest following intranasal drip and the longest following subcutaneous injection. The longest residence time was associated with subcutaneous injection, while the highest peak concentration was observed after nasal drip, and the lowest peak concentration was seen after subcutaneous injection, aligning with the absorption characteristics of the parent drug. There were no significant differences in overall exposure and product conversion rate.

Table 7. Main pharmacokinetic parameters of AC-279 after administration of pimavanserin tartrate 3 mg/kg via different routes (Mean ± SD, n = 6).

Parameters	Unit	i. n.	i. m.	s. c.
$t_{1/2}$	h	1.59 ± 0.74	1.63 ± 0.52	1.99 ± 0.46
T_{max}	h	0.40 ± 0.14	0.46 ± 0.1	0.70 ± 0.27
C_{max}	nM	9.77 ± 3.45	8.48 ± 2.65	5.65 ± 1.06*
$AUC_{(0-t)}$	h × nM	15.95 ± 8.12	14.75 ± 8.65	14.39 ± 1.67
$AUC_{(0-t)}$	h × nM	20.35 ± 9.70	20.02 ± 9.41	19.60 ± 1.62
$MRT_{(0-t)}$	h	2.11 ± 0.73	2.62 ± 0.69	4.50 ± 1.05
$AUC_{(0-t,\ AC-279)}/AUC_{(0-t,\ ACP-103)}$	%	2.56 ± 1.33	2.42 ± 1.70	3.17 ± 0.64

*P < 0.05, same dose compared with nasal drip.

4. Discussion

ACP-103, a medication for the treatment of PDP, is currently available as an oral drug, which does not adequately address the clinical needs of elderly PDP patients. To develop formulations suitable for intranasal, intramuscular, and subcutaneous administration, corresponding pharmacokinetic studies are necessary. Since mice are the animal model used for PDP pharmacodynamic studies [20], this study compared the pharmacokinetic profiles of varying doses of ACP-103 administered through nasal drip, intramuscular injection, and subcutaneous injection in mice.

It is known that AC-279 is the active metabolite of ACP-103 [17], hence this paper established an LC-MS/MS method for the simultaneous determination of ACP-103 and AC-279 concentrations in mouse plasma. This method, characterized by its simplicity, speed, and sensitivity, has been successfully applied to the pharmacokinetic study of ACP-103 in mice.

Before developing a method for the simultaneous quantification of ACP-103 and AC-279, it was essential to determine their quantitative linear ranges to accurately depict their in vivo processes. Ezzeldin E *et al.* [21] have reported a UPLC-MS/MS method for quantifying ACP-103 in mouse brain tissue for brain distribution studies. Shixiao Wang *et al.* [22] developed a UPLC-MS/MS method for quantifying ACP-103 in rat plasma, but with a limited quantification range of 1 - 80 ng/mL. Tingting Ma *et al.* [23] established an LC-MS/MS method for determin-

ing ACP-103 in Beagle plasma, with a sample analysis time of 4.5 minutes, which is less efficient. None of these methods were designed for the simultaneous quantification of the active metabolite AC-279. This study optimized an LC-MS/MS method for the simultaneous determination of ACP-103 and AC-279, finding that the best chromatographic peak shape was achieved using acetonitrile precipitation for protein removal. To effectively eliminate proteins and endogenous interferences from plasma, a six-fold volume of acetonitrile was used for protein precipitation. Chromatographic separation was carried out on a C18 column with a mobile phase of water (containing 0.1% formic acid) and methanol (containing 0.1% formic acid) using gradient elution. The analysis time for each sample was reduced to just 3 minutes, enhancing detection efficiency. Additionally, no cross-interference was observed despite the close retention times of ACP-103 and AC-279 (ACP-103 at 1.64 minutes and AC-279 at 1.63 minutes). The methodology was validated to satisfy the requirements of the pharmacokinetic study.

In this study, ACP-103 demonstrated an exceptionally rapid absorption rate in mice following administration via three distinct routes, with minimal inter-individual variability. This characteristic is a significant advantage in addressing the challenges of dysphagia in critically ill patients and the substantial inter-individual differences observed in oral administration in humans. The intranasal administration route exhibited the highest drug exposure (C_{max}) and the shortest time to peak concentration (T_{max}), primarily attributed to the unique physiological structure of the nasal mucosa. The nasal mucosa is characterized by a rich vascular network and a large surface area, allowing drugs administered intranasally to rapidly pass through the mucosal epithelial cells and enter the systemic circulation, thereby bypassing the hepatic first-pass effect and significantly enhancing the drug's bioavailability. Additionally, the ciliary movement and mucus layer on the nasal mucosa further facilitate the rapid absorption of the drug. In contrast, the intramuscular administration route benefits from the high vascular density and ample blood supply in muscle tissue. Once the drug diffuses from the injection site into the surrounding tissue, it can promptly enter the bloodstream via capillaries. On the other hand, the subcutaneous administration route demonstrates the lowest drug exposure and the longest residence time in the body, due to the relatively low vascular density and slower blood flow in subcutaneous tissue, which prolongs the time required for the drug to enter the systemic circulation from the injection site.

The generation rate and exposure of AC-279 varied significantly among differences administration routes. Under the intranasal administration route, AC-279 demonstrated the fastest generation rate and the shortest time to peak concentration (T_{max}), whereas under the subcutaneous injection route, its generation rate was the slowest, and the T_{max} was the longest. This phenomenon was consistent with the absorption characteristics of the parent drug, ACP-103, indicating that the generation rate of AC-279 was closely related to the absorption rate of ACP-103. In the case of intranasal administration, ACP-103 rapidly entered the systemic circulation, thereby accelerating its conversion in the liver and other metabolic tissues to

generate AC-279. In contrast, under the subcutaneous injection route, the slower absorption rate of ACP-103 resulted in a corresponding reduction in the generation rate of AC-279. As an active metabolite of ACP-103, AC-279 may possess similar or even stronger 5-HT_{2A} receptor antagonistic effects compared to the parent drug, thereby enhancing the antipsychotic efficacy of the treatment. Under the intranasal administration route, the rapid generation of AC-279 may contribute to the swift alleviation of hallucinations and delusions in patients with Parkinson's disease psychosis (PDP). Furthermore, the intranasal administration route exhibited the highest product conversion rate for AC-279, while the subcutaneous injection route showed the lowest conversion rate. This phenomenon may be related to the metabolic pathways and enzyme activities of ACP-103 under different administration routes. Under intranasal administration, the rapid absorption of ACP-103 may accelerate its metabolic rate in the liver, thereby increasing the generation of AC-279. In contrast, under subcutaneous injection, the slower absorption of ACP-103 may reduce its metabolic rate in the liver, leading to a decrease in the generation of AC-279.

The intranasal administration route does not require swallowing, making it particularly suitable for elderly PDP patients with dysphagia, thereby improving medication adherence. The intramuscular injection route is well-suited for hospitalized patients, especially those requiring long-term monitoring and treatment for PDP. The subcutaneous injection route is ideal for home care settings, particularly for PDP patients who need long-term treatment and cannot frequently visit healthcare facilities. Compared to traditional oral administration, the intranasal, intramuscular, and subcutaneous administration routes offer significant advantages in terms of drug absorption rate, bioavailability, and drug release stability. These findings provide crucial insights for the development of pimavanserin dosage forms, particularly for personalized treatment strategies targeting elderly patients with Parkinson's disease psychosis.

In conclusion, this study successfully developed a new LC-MS/MS method for the simultaneous quantification of ACP-103 and its active metabolite AC-279 in mouse plasma. This method is marked by its straightforward operation, high sensitivity, and suitability for rapid detection of drug concentrations in mouse plasma. The pharmacokinetic profiles of nasal drip, intramuscular injection, and subcutaneous injection exhibited some differences, with higher exposure observed after nasal drip and intramuscular injection of ACP-103, and slightly lower exposure following subcutaneous injection.

Conflicts of Interest

The authors declare no conflicts of interest regarding the publication of this paper.

References

[1] Gątarek, P., Pawełczyk, M., Jastrzębski, K., Głąbiński, A. and Kałużna-Czaplińska, J. (2019) Analytical Methods Used in the Study of Parkinson's Disease. *TrAC Trends in Analytical Chemistry*, **118**, 292-302. https://doi.org/10.1016/j.trac.2019.05.047

[2] Lees, A.J., Hardy, J. and Revesz, T. (2009) Parkinson's Disease. *The Lancet*, **373**, 2055-2066. https://doi.org/10.1016/s0140-6736(09)60492-x

[3] Parkinson's Disease and Movement Disorders Group of the Neurology Section of the Chinese Medical Association, Parkinson's Disease and Movement Disorders Group of the Neurologists Branch of the Chinese Physicians Association (2020) Chinese Parkinson's Disease Treatment Guidelines (Fourth Edition). *Chinese Journal of Neurology*, **53**, 973-986.

[4] Agustín-Pavón, C., Braesicke, K., Shiba, Y., Santangelo, A.M., Mikheenko, Y., Cockroft, G., *et al.* (2012) Lesions of Ventrolateral Prefrontal or Anterior Orbitofrontal Cortex in Primates Heighten Negative Emotion. *Biological Psychiatry*, **72**, 266-272. https://doi.org/10.1016/j.biopsych.2012.03.007

[5] Bari, A. and Robbins, T.W. (2013) Inhibition and Impulsivity: Behavioral and Neural Basis of Response Control. *Progress in Neurobiology*, **108**, 44-79. https://doi.org/10.1016/j.pneurobio.2013.06.005

[6] Izquierdo, A. (2017) Functional Heterogeneity within Rat Orbitofrontal Cortex in Reward Learning and Decision Making. *The Journal of Neuroscience*, **37**, 10529-10540. https://doi.org/10.1523/jneurosci.1678-17.2017

[7] Carli, M. and Samanin, R. (1992) Serotonin2 Receptor Agonists and Serotonergic Anorectic Drugs Affect Rats' Performance Differently in a Five-Choice Serial Reaction Time Task. *Psychopharmacology*, **106**, 228-234. https://doi.org/10.1007/bf02801977

[8] Patra, S. (2016) Return of the Psychedelics: Psilocybin for Treatment Resistant Depression. *Asian Journal of Psychiatry*, **24**, 51-52. https://doi.org/10.1016/j.ajp.2016.08.010

[9] Daniel, J. and Haberman, M. (2017) Clinical Potential of Psilocybin as a Treatment for Mental Health Conditions. *Mental Health Clinician*, **7**, 24-28. https://doi.org/10.9740/mhc.2017.01.024

[10] Evenden, J.L. and Ryan, C.N. (1999) The Pharmacology of Impulsive Behaviour in Rats VI: The Effects of Ethanol and Selective Serotonergic Drugs on Response Choice with Varying Delays of Reinforcement. *Psychopharmacology*, **146**, 413-421. https://doi.org/10.1007/pl00005486

[11] Robbins, T. (2002) The 5-Choice Serial Reaction Time Task: Behavioural Pharmacology and Functional Neurochemistry. *Psychopharmacology*, **163**, 362-380. https://doi.org/10.1007/s00213-002-1154-7

[12] Zhang, J.Z. (2016) Overview of New Drugs Approved by FDA in April 2016. *Shanghai Medicine*, **37**, 81.

[13] Hawkins, T. and Berman, B.D. (2017) Pimavanserin: A Novel Therapeutic Option for Parkinson Disease Psychosis. *Neurology Clinical Practice*, **7**, 157-162. https://doi.org/10.1212/cpj.0000000000000342

[14] Cruz, M.P. (2017) Pimavanserin (Nuplazid): A Treatment for Hallucinations and Delusions Associated with Parkinson's Disease. *Pharmacology & Therapeutics*, **42**, 368-371.

[15] Forman, M., Kouassi, A., Brandt, T., Barsky, L., Zamora, C. and Dekarske, D. (2021) Palatability and Swallowability of Pimavanserin When Mixed with Selected Food Vehicles: An Exploratory Open-Label Crossover Study. *Geriatrics*, **6**, Article 61. https://doi.org/10.3390/geriatrics6020061

[16] Zhong, Z. (2022) Analysis of Oral Motor Symptoms in Parkinson's Disease and Their Influencing Factors. Master's Thesis, Nanchang University.

https://doi.org/10.27232/d.cnki.gnchu.2022.000666

[17] Wojtasik-Bakalarz, K. and Siwek, M. (2023) New Antipsychotic Medication. *Pharmacotherapy in Psychiatry and Neurology*, **39**, 19-38. https://doi.org/10.5114/fpn.2022.124608

[18] International Council for Harmonisation of Technical Requirements for Pharmaceuticals for Human Use (2022) ICH.ICH M10: Bioanalytical Method Validation and Study Sample Analysis.

[19] U.S. Food and Drug Administration (2003) Guidance for Industry: Bioavailability and Bioequivalence Studies for Orally Administered Drug Products—General Considerations. U.S. Department of Health and Human Services.

[20] Zhu, H.L., Zhou, P.L., Fu, F.H. and Su, R.B. (2022) Advances in the Study of Signaling Pathways Activated by Hallucinogens to Produce Hallucinogenic. *Chinese Pharmacological Bulletin*, **38**, 1607-1612.

[21] Ezzeldin, E., Iqbal, M., Asiri, Y.A., Ali, A.A. and El-Nahhas, T. (2020) A Rapid, Simple and Highly Sensitive UPLC-MS/MS Method for Quantitation of Pimavanserin in Plasma and Tissues: Application to Pharmacokinetics and Brain Uptake Studies in Mice. *Journal of Chromatography B*, **1143**, Article 122015. https://doi.org/10.1016/j.jchromb.2020.122015

[22] Wang, S., Wang, Y., Gao, S., Zhang, Y., Wang, H., Zhao, L., *et al*. (2017) Development of a UPLC-MS/MS Method for Determination of Pimavanserin Tartrate in Rat Plasma: Application to a Pharmacokinetic Study. *Journal of Pharmaceutical Analysis*, **7**, 406-410. https://doi.org/10.1016/j.jpha.2017.07.004

[23] Ma, T.T., Zuo, L. and Chen, J. (2020) Determination of Plasma Concentrations of Pimavanserin in Beagle Dogs by LC-MS/MS and Pharmacokinetic Study. *Journal of Pharmaceutical Research*, **39**, 22-26. https://doi.org/10.13506/j.cnki.jpr.2020.01.005